

Study on Advanced Construction Method Application to NPPs Loading Tests of SC Shear Wall for Advanced Construction Methods PART 2 Connection method between SC wall and foundation slab

**Shimpei Takamura¹, Shinji Takami², Masaki Yukawa³,
Toshiaki Hamagami⁴, Shinya Kita⁵, Hiroki Iwahashi⁶**

¹ Staff Member, Obayashi Corporation, Tokyo, Japan (takamura.shimpei@obayashi.co.jp)

² Deputy General Manager, Obayashi Corporation, Tokyo, Japan

³ Manager-in-Charge, Obayashi Corporation, Tokyo, Japan

⁴ General Manager, Obayashi Corporation, Tokyo, Japan

⁵ Senior Engineer, Mitsubishi Heavy Industries, Ltd., Hyogo, Japan

⁶ Manager, Kansai Electric Power Co., Inc, Osaka, Japan

ABSTRACT

In order to apply the use of steel plate reinforced concrete (SC) structures in Japanese nuclear power plants, advanced construction methods are developed to minimize the construction term. In this study, horizontal loading tests were conducted on seismic wall specimens to understand the mechanical performance of the method by rebar connection between SC wall and basement. The load-bearing capacity of rebar connection between SC wall and basement was found to be lower than that of embedded plates between SC wall and basement. The Japanese SC structural design code (JEAC4618) does not provide a design method to reasonably evaluate the seismic performance of the rebar type. Therefore, a study of a load capacity evaluation method was conducted, and a design formula was proposed to properly evaluate the load characteristics.

INTRODUCTION

In order to reduce the construction term of SC structures. We consider that it is effective to develop methods that rationalize (a) "connection of faceplates between SC blocks" and (b) "rebar connection of SC wall and basement" will be effective in reducing the construction term. It is necessary to develop the design method for their practical use. However, there have been few previous experiments on them, and their structural characteristics have not yet been clarified. Therefore, we conducted horizontal load tests on earthquake-resistant walls to understand their mechanical performance. In this paper, we report the details and results of the experiments on "Rebar connection" shown in Figure 1. This type uses rebars to anchor the SC to the foundation concrete, which shortens the construction term compared to the embedment and anchoring types. However, the rebar type exhibits inferior seismic performance in comparison to the embedment or anchoring types, but JEAC 4618¹⁾ does not provide specific design methods, such as a formula for setting up a restoring model. The experimental results of the type described in (a) are reported in specimens No.1-4 of PART1 (see Ref. ²⁾).

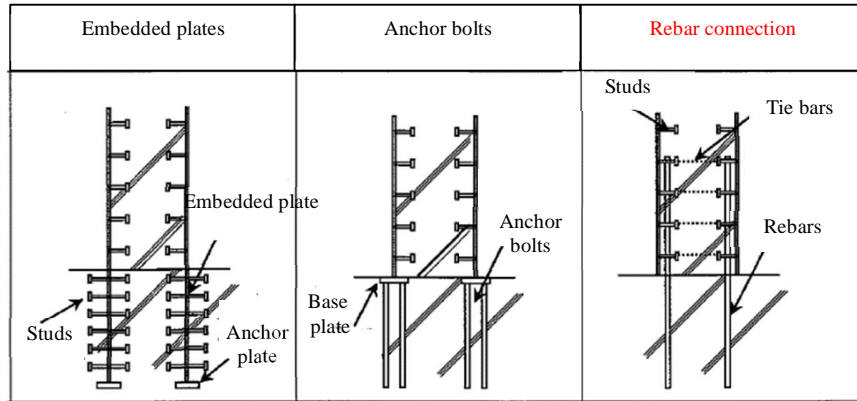


Figure 1: Connection types at a bottom of SC wall to basement by (JEAC4618)

CONFIRMATORY TEST PLAN

The two specimens which are approximately one-fifth the size of full-scale buildings are shown in Table 1 and Figure 2. The specimen “No. 1” corresponds to embedded type (see Ref. ²⁾). The specimen “No. 5” corresponds to the Rebar type. The web section of No. 5 has a wall thickness of 230 mm, a steel plates of PL 2.3, and studs with a diameter of 4φ (spacing of @70mm(vertical) and @60mm(horizontal)). The flange section has a wall thickness of 115 mm, a steel plates of PL 6.0, and the studs with a diameter of 6φ (spacing of @70mm(vertical) and @45mm(horizontal)). For No. 5, the diameter of rebar anchored to the lower stub is D16 for the web and D19 for the flange, and each rebar is embedded to depths that does not cause bond failure. Prior to the concrete pouring to the SC wall, the concrete joint area on the top surface of the lower stub (hereinafter, horizontal joint area) was roughened as shown in Figure 3. For the No. 5, the amount of reinforcement of rebar is lower than that of the SC steel plates for the horizontal cross section of the wall. The bending capacity is determined by the yield of rebar, and the calculated capacity is lower than that of No. 1. The shear span ratio was set to 0.7 for both specimens, and no vertical axial force was applied. The loading device (see Figure 4) utilised a hydraulic jack is used to apply a repetitive positive-negative horizontal force to the force stub at the upper stub on the wall. Figure 5 shows the loading program.

Table 1: A list of specimens

Specimen name	Connection type at a bottom of SC wall to basement	Web plate	Flange plate	Rebar	Tie bar
No.1	Embedded type	PL2.3	PL6.0	—	—
No.5	Rebar type			Web D16, @120 Flange D19, @90	Web φ 4mm, @70,60 Flange φ 6mm, @70,45

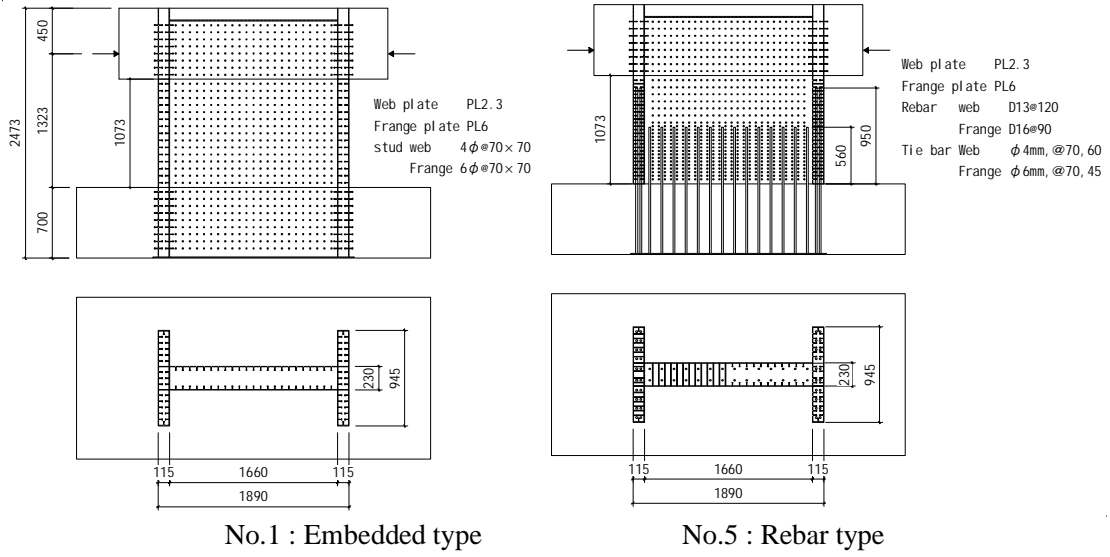


Figure 2: Test specimens



Figure 3: Roughness of concrete joint surfaces of horizontal joint area (No. 5)

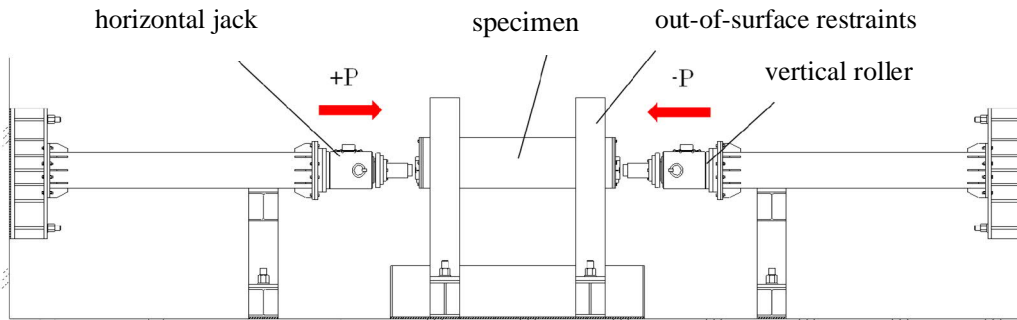


Figure 4: Diagram of the loading device

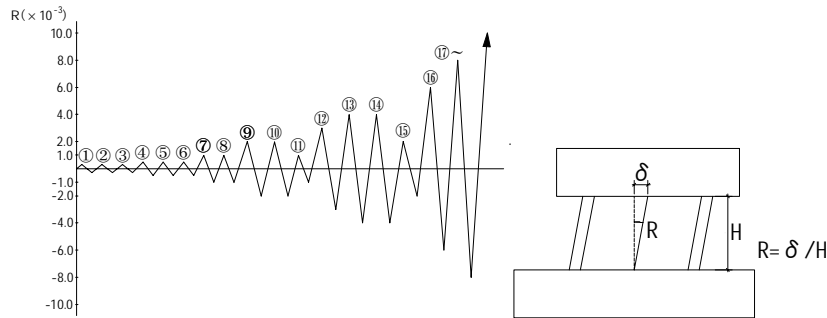


Figure 5: The loading program

CONFIRMATORY TEST RESULTS

Table 2 shows the mechanical properties of the materials. Figure 6 shows the specimens after loading test, and the test results are shown in Figure 7 to Figure 9.

Specimen No.1

After crack initiation, the web steel plate yielded first, then the flange steel plate yielded, finally the shear failure occurred, and the maximum load was recorded. The horizontal component angle at the maximum load was 8.0/1000 rad. No rupture of the steel plate occurred until the end, but the web steel plate exhibited buckling due to shear deformation. The load-total displacement relationship was found to be stable.

Specimen No.5

After crack initiation, the web steel plate yielded first, the flange rebar yielded in bending next, then the web rebar yielded in bending, and in the subsequent cycle, a horizontal slip obviously occurred in the horizontal joint area. A temporary load drop occurred after the slip, but the load increased again (Figure 8). As the overall deformation increased, the percentage of the slip deformation increased. The deformation was very large (49.9/1000 rad.) when the maximum load was applied, but the load-overall displacement relationship was generally stable until the end. During the final cycle, the steel plate ruptured at the bottom of the flange on the compression side due to sliding deformation and buckling occurred at the web corner on the compression side due to deformation concentration caused by sliding. However, the steel plate did not buckle in other areas of the web section. The failure mode was slippage in the horizontal joint area. Figure 9 shows a comparison of the load-shear strain relationship. The initial stiffness is shown to be similar for both specimens, but the maximum load is lower for No. 5. The shear strain at the maximum load is approximately 7000 μ for No. 1, while No. 5 does not drop to 8900 μ (No. 5 was measured up to 8900 μ because the displacement gauge was removed before the maximum load). Consequently, Rebar type has lower shear strength than that of Embedded types, but the ultimate shear strain is higher, thus the toughness against shear deformation can be expected.

Table 2-1: Mechanical properties of materials (concrete)

		Compressive strength (N/mm ²)	Splitting strength (N/mm ²)	Young's modulus ($\times 10^4$ N/mm ²)	Poisson's ratio
Concrete (Wall)	No.1	38.1	3.00	2.69	0.195
	No.5	30.1	2.29	2.44	0.180

Table 2-2: Mechanical properties of materials (steel)

	Yield strength (N/mm ²)	Yield point strain	Young's modulus ($\times 10^5$ N/mm ²)	Tensile strength (N/mm ²)	Poisson's ratio
PL2.3(Web, Splice plate)	310	1549 μ	2.09	449	—
PL6.0(Flange)	333	1927 μ	2.04	474	
D16(Web)	380	2181 μ	1.96	582	
D19(Flange)	362	1976 μ	1.99	545	
Stud 4 ϕ (Web)	510	—	—	532	
Stud 6 ϕ (Flange)	539	—	—	568	

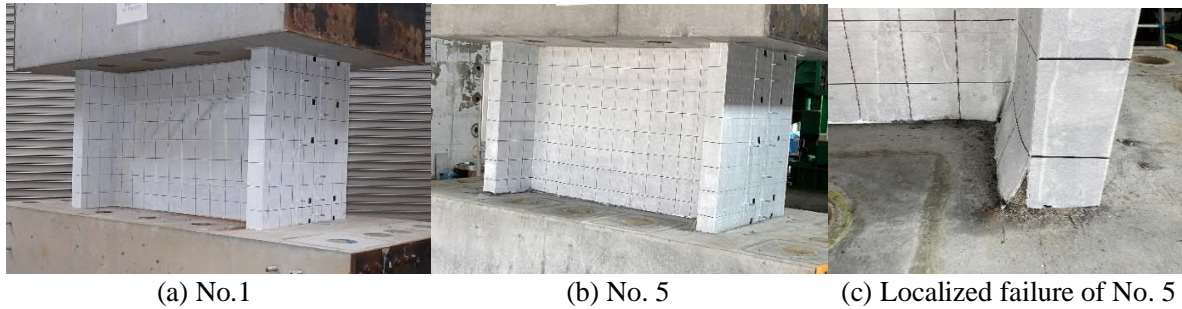


Figure 6: Final failure mode of specimens

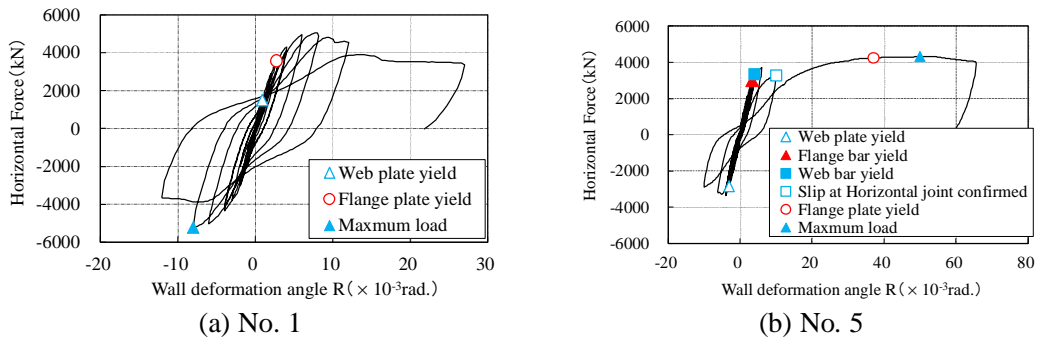


Figure 7: Load- wall deformation angle relations

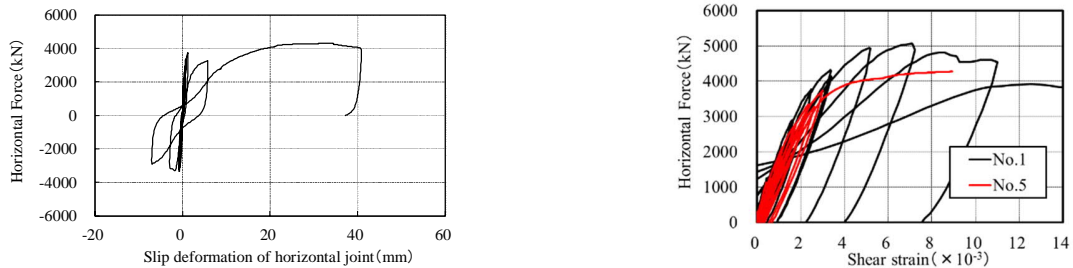


Figure 8: Slip deformation of the horizontal joint (No. 5)

Figure 9: Load-Shear Strain Relationship

DESIGN METHOD CONSIDERATION

Slip Capacity of Horizontal Joints

In case of slip in a horizontal joint area, the load capacity of the whole wall cannot be utilized. In addition, as the load decreases, the restoring force curve becomes a slip shape with a small loop area, thus the seismic resistance of the structure is lowered. We evaluated the slip resistance of Rebar type by using the following evaluation method by Wada et al³⁾ (hereinafter “Wada formula”).

$$\left(\frac{M_j}{M_u}\right)^2 + \left(\frac{Q_j}{Q_{stu}}\right)^2 = 1 \quad (1)$$

$$Q_{stu} = A_{all} [14.1 + 0.8(p_{jy} \cdot \sigma_{jy} + \sigma_o)] \quad (2)$$

Where A_{all} is total wall cross sectional area, M_j is bending moment at the bottom of wall, M_u is bending ultimate strength, Q_j is shear force, p_{jy}, σ_{jy} is ratio of rebar to inserted bar x yield strength (both are equivalent averages of web and flange), σ_o is axial stress.

Because Wada formula is used to evaluate the maximum load capacity after slippage, we added the case of lower slippage capacity by multiplying Wada formula by 0.8.

As illustrated in Table 3 and Figure 10, the experimental and calculated values for the specimens^{3),4),5)} that failed due to sliding are presented, in addition to this specimen. The experimental/calculated values of the original formula tended to slightly overestimate the bearing capacity, ranging from 0.90 to 1.02. However, the experimental/calculated values of the Wada formula x 0.8 resulted in a conservative evaluation of 1.13 to 1.28.

Table 3: experimental and calculated values at the onset of the slip (including previous specimens^{3),4)})

specimen	No. 5	Previous test 1	Previous test 2	Previous test 3
Test result*1 (kN)	3732	4661	2959	4498
Wada formula*2 (kN)	4143	5170	2895	4840
0.8×Wada formula*3 (kN)	3314	4136	2316	3872
*1/*2	0.90	0.90	1.02	0.93
*1/*3	1.13	1.13	1.28	1.16

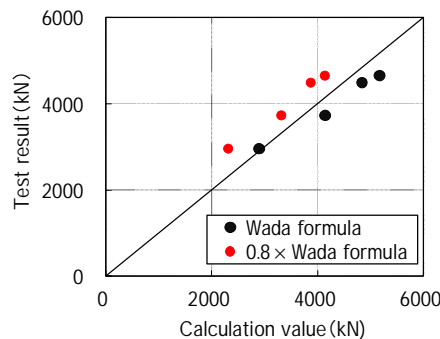


Figure 10: Conformity of calculated slip generation values (including previous specimens^{3),4)})

Restoring model of load-shear strain relationship ($Q-\gamma$)

Even though JEAC4618 provides calculation formulas for the $Q-\gamma$ model for Embedded type and anchor type, it does not provide a reasonable model for Rebar type. Therefore, a modelling study of the $Q-\gamma$ relationship was conducted based on JEAC4618 and the model of JEAC4601⁶⁾ for RC structures. The models for the three cases compared with experimental values are shown below.

Case 1: JEAC 4618

First break point: Crack point of concrete

$$Q_1 = \left(A_c + \frac{G_s}{G_c} \cdot A_s \right) \cdot \tau_{cr} \quad (N) \quad (3)$$

$$\gamma_1 = \frac{\tau_{cr}}{G_c} \quad (rad) \quad (4)$$

$$\tau_{cr} = \sqrt{(0.31\sqrt{\sigma_B} \cdot (0.31\sqrt{\sigma_B} + \sigma_V))} \quad (N) \quad (5)$$

Second break point: Yield point of steel plate

$$Q_2 = \frac{K_\alpha + K_\beta}{\sqrt{(3K_\alpha^2 + K_\beta^2)}} \cdot A_s \cdot \sigma_y \quad (N) \quad (6)$$

$$\gamma_2 = \frac{Q_2}{K_\alpha + K_\beta} \quad (rad) \quad (7)$$

$$K_\alpha = A_s \cdot G_s \quad (8)$$

$$K_\beta = \frac{1}{\frac{4}{A_c E_c} + \frac{2(1-\nu_s)}{A_s + E_s}} \quad (9)$$

Third break point: Ultimate point.

$$Q_3 = A_c \sqrt{\left(\left(\frac{A_s \cdot \sigma_y}{A_c} \right) \cdot \nu_1 \cdot \sigma_B \right)} \quad (N) \quad (10)$$

$$\gamma_3 = 6.0 \times 10^{-3} \quad (rad) \quad (11)$$

Where A_c, A_s is shear cross section of concrete and steel plate, G_c, G_s is shear stiffness of concrete and steel plate, σ_B is compressive strength of concrete, σ_V is vertical axial stress considering steel plate, σ_y is yield strength of steel sheet, E_c, E_s is young's modulus of concrete and steel plate, ν_s is poisson's ratio of steel plate.

Case 2: JEAC 4601

First break point: Crack point of concrete

$$Q_1 = A_c \sqrt{0.31 \sqrt{F_c} (0.31 \sqrt{F_c} + \sigma_V)} \quad (N) \quad (12)$$

$$\gamma_1 = Q_1 / A_c G \quad (rad) \quad (13)$$

Second break point: Yield point

$$Q_2 = 1.35 Q_1 \quad (N) \quad (14)$$

$$\gamma_2 = 3\gamma_1 \quad (rad) \quad (15)$$

Third break point: Ultimate point.

$$Q_3 = A_c \left\{ \left[1 - \frac{\tau_s}{(1.4\sqrt{F_c})} \right] \tau_o + \tau_s \right\} \quad (N), \quad (\tau_s \leq 1.4\sqrt{F_c}) \quad (16)$$

$$Q_3 = 1.4 A_c \sqrt{F_c} \quad (N), \quad (\tau_s > 1.4\sqrt{F_c}) \quad (17)$$

$$\gamma_3 = 0.004 \quad (rad) \quad (18)$$

$$\tau_o = (0.67 - 0.4M/QD) \times 1.4\sqrt{F_c} \quad (19)$$

$$\tau_s = \frac{(P_V + P_H)\sigma_{wy}}{2} + \frac{(\sigma_V + \sigma_H)}{2} \quad (20)$$

Where F_c is compressive strength of concrete, G is shear stiffness of concrete, σ_V, σ_H is vertical and horizontal axial stress, M/QD is shear span ratio, P_V, P_H is ratio of vertical and horizontal bar, σ_{wy} is rebar yield stress.

Case 3: Modified model of JEAC4618

The first breaking point (Q_1, γ_1), the second breaking point (Q_2, γ_2), and the third breaking point γ_3 are equivalent to those observed in Case 1.

Equation (10) illustrates the shear resistance of truss mechanism, whereby the tension member, which constitute the balance of forces, are assigned the yield capacity of the web steel plate. Conversely, in the case of the Rebar type, the resistance of the tension member is supposed to be limited by the resistance force of the yielding of the web steel plate, the yielding of the web rebar and the failure of the anchorage due to the adhesion of the web rebar, and the ultimate shear capacity is determined by the minimum value of these three factors. Consequently, Q_3 of the Rebar type is evaluated using Equation (10') through instead of Equation (10).

$$Q_3 = A_c \sqrt{\left(\left(\frac{\min(A_s \cdot \sigma_y, A_{bw} \cdot \sigma_{ybw}, A_{bw} \cdot \sigma_{bow})}{A_c} \right) \cdot v_1 \cdot \sigma_B \right)} \quad (N) \quad (10')$$

$$\sigma_{bow} = \tau_b \cdot \varphi \cdot \frac{L_b}{A_b} \quad (21)$$

$$\tau_b = \max (\tau_{co}/1.5, \tau_u/1.2) \quad (22)$$

$$\tau_{co} = 0.31m(0.33 - 0.047\alpha)\sqrt{F_c} \text{ (Rebar D38 or less)} \quad (23)$$

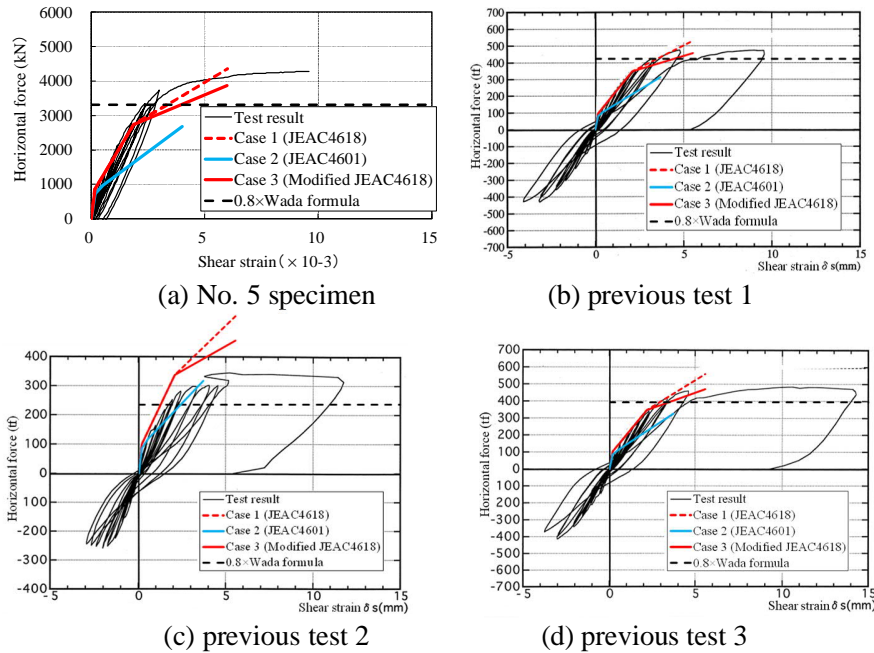
$$\tau_u = 0.31m(0.31 - 0.02\alpha + 15.2p_w)\sqrt{F_c} \text{ (} p_w \geq 0.001 \text{)} \quad (24)$$

$$\tau_u = 0.31m \cdot p_w(325 - 20\alpha)\sqrt{F_c} \text{ (} p_w < 0.001 \text{)} \quad (25)$$

Where A_{bw} is total cross-sectional area of rebar, σ_{ybw} is yield strength of rebar, $\sigma_{b_{ow}}$ is rebar stress at bond splitting failure of rebar, τ_b is bond strength of rebar, φ is rebar circumference, L_b is joint length between steel plate and rebar, A_b is cross-sectional area of a single rebar, m is ratio of clearance between bars to nominal diameter of bars (≤ 7), d_b is nominal diameter of rebar, p_w is out-of-plane reinforcing steel ratio (tie-bar ratio).

Comparison of experimental and calculated values

Figure 11 shows a comparison of the calculated values of the Q- γ relationship for the No. 5 and the previous rebar type specimens. The calculated value of the slip generated load (Wada formula x 0.8) is also shown in the figure. Of the previous specimens, previous test 1 through 3 reached failures due to slip failure of the horizontal joints, while previous test 4 and 5 were reported to have failed due to shear failure. Case 2 exhibited the lowest load, resulting in significant underestimation for previous test 4 and 5, which failed in shear, resulting in a poor fit. Conversely, the load in Case 3 is lower than in Case 1, aligning with the experimental findings demonstrating that Rebar type has a reduced maximum load compared to the embedded type. Case 3 is the best fit, which can be judged by looking at the compatibility with the experimental values up to the onset of slip loading for the slip failed specimens and up to the end point for the shear failed specimens.



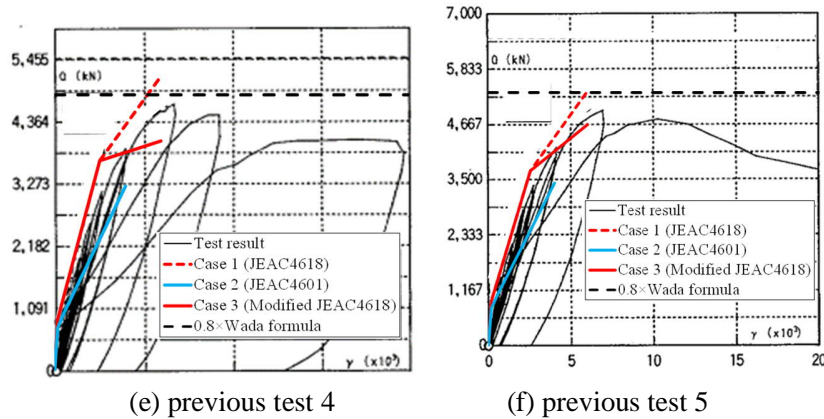


Figure 11: Comparison of calculated results with test results (Q- γ)

CONCLUSION

Rebar type was selected as a rationalization technique to shorten the construction term of SC structures. The horizontal load tests were conducted on a specimen of seismic-resistant wall to understand its mechanical properties and to develop a design method. The test specimen failed due to slipping in the horizontal joint area; the SC wall anchorage to the foundation concrete is a weak point of the Rebar type. However, an effective evaluation method for the slippage strength was obtained. Additionally, a novel calculation method for the restoring model of Q- γ for the Rebar type was proposed by modifying the method by JEAC4618.

ACKNOWLEDGEMENT

This study was carried out by The Kansai Electric Power Co., Inc., Hokkaido Electric Power Co., Inc., Shikoku Electric Power Co., Inc., Kyushu Electric Power Co., Inc., The Japan Atomic Power Co., The Institute of Applied Energy, Mitsubishi Heavy Industries, Ltd., Obayashi Corp., Taisei Corp. and Takenaka Corp. with the Ministry of Economy, Trade and Industry (METI) subsidy.

REFERENCES

- 1) Japan Electric Association, Japan Electric Association Code JEAC4618-2009.
- 2) Masaki Yukawa. et al. (2025), “Study on Advanced Construction Method Application to NPPs Loading Tests of SC Shear Wall for Advanced Construction Methods PART 1 Comparison of faceplate connecting methods” SMiRT 28, Canada, August.
- 3) Wada, Y., et al. (2001), “Study on Steel Plate Reinforced Concrete Structure Part.8 Shear Test of SC Shear Wall with joint bars” SUMMARIES OF TECHNICAL PAPERS OF ANNUAL MEETING, ARCHITECTURAL INSTITUTE OF JAPAN, NO.21488.
- 4) Kawashima, M., et al. (2001), “Study on Steel Plate Reinforced Concrete Structure Part.9 Evaluation Method for Shear Deformation of SC Shear Walls” SUMMARIES OF TECHNICAL PAPERS OF ANNUAL MEETING, ARCHITECTURAL INSTITUTE OF JAPAN, NO.21488.
- 5) Adachi, et al. (1999), “Shear Tests on Anchorage Rebars of SC Wall (Outline of the Experimental and the Results)” SUMMARIES OF TECHNICAL PAPERS OF ANNUAL MEETING, ARCHITECTURAL INSTITUTE OF JAPAN, NO.21626.
- 6) Japan Electric Association, Japan Electric Association Code JEAC4601-2008.